HHS Public Access

Author manuscript

*Cell Rep*. Author manuscript; available in PMC 2022 July 10.

Published in final edited form as:

*Cell Rep*. 2022 June 28; 39(13): 110990. doi:10.1016/j.celrep.2022.110990.

# Development of allergen-specific IgE in a food-allergy model requires precisely timed B cell stimulation and is inhibited by Fgl2

**Qiang Chen**[1], **Markus Xie**[1], **Hong Liu**[1], **Alexander L. Dent**[1,2,*]

[1]Department of Microbiology and Immunology, Indiana University School of Medicine, Indianapolis, IN, USA

[2]Lead contact

## SUMMARY

Immunoglobulin E (IgE) responses are a central feature of allergic disease. Using a well-established food-allergy model in mice, we show that two sensitizations with cognate B cell antigen (Ag) and adjuvant 7 days apart promotes optimal development of IgE+ germinal center (GC) B cells and high-affinity IgE production. Intervals of 3 or 14 days between Ag sensitizations lead to loss of IgE+ GC B cells and an undetectable IgE response. The immunosuppressive factors Fgl2 and CD39 are down-regulated in T follicular helper (TFH) cells under optimal IgE-sensitization conditions. Deletion of *Fgl2* in TFH and T follicular regulatory (TFR) cells, but not from TFR cells alone, increase Ag-specific IgE levels and IgE-mediated anaphylactic responses. Overall, we find that Ag-specific IgE responses require precisely timed stimulation of IgE+ GC B cells by Ag. Furthermore, we show that Fgl2 is expressed by TFH cells and represses IgE. This work has implications for the development and treatment of food allergies.

## Graphical Abstract



*Correspondence: adent2@iupui.edu.

AUTHOR CONTRIBUTIONS

Conceptualization, A.L.D. and Q.C.; methodology, A.L.D. and Q.C.; investigation, A.L.D., Q.C., M.X., and H.L.; writing – original draft, A.L.D. and Q.C.; writing – review & editing, A.L.D., Q.C., M.X., and H.L.; funding acquisition, A.L.D.; supervision, A.L.D.

SUPPLEMENTAL INFORMATION

Supplemental information can be found online at https://doi.org/10.1016/j.celrep.2022.110990.

DECLARATION OF INTERESTS

The authors declare that they have no relevant conflicts of interest.

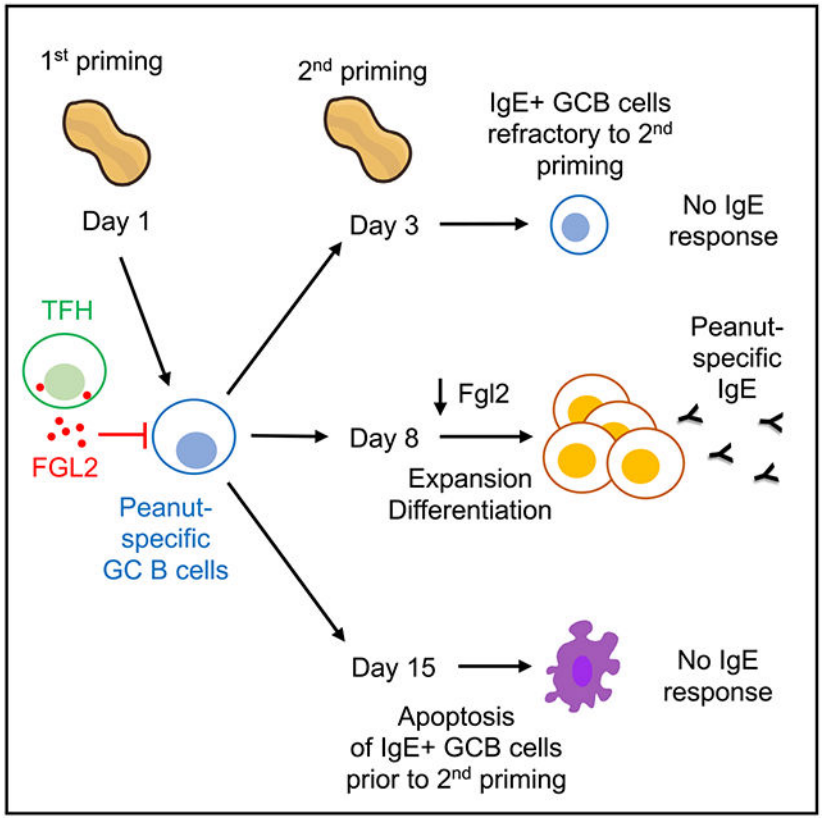



## In brief

Using a mouse food-allergy model, Chen et al. find that allergen-specific IgE responses require precisely timed stimulation of IgE+ germinal center B cells. The authors further show that Fgl2 expressed by T follicular helper cells represses IgE. This work has implications for the development and treatment of food allergy.


## INTRODUCTION

Food allergy is a pathologic response of the immune system triggered by food antigens (Ags). The prevalence of food allergy has been increasing since the 1990s as part of the second wave of the allergy epidemic (Asher et al., 2006; Yu et al., 2016), and it is estimated that up to 8% of children are affected by a food allergy in the United States (Tordesillas et al., 2017). One of the most important categories of food allergy is immunoglobulin E (IgE)-mediated immediate hypersensitivity reactions, as cross-linking of allergen-specific IgE bound to mast cells induces severe immune responses including anaphylaxis (Gould and Ramadani, 2018; Gould et al., 2003).

Despite its critical role in mediating allergic disease, we are just beginning to understand the mechanism of IgE regulation *in vivo*. Like the other Ig isotypes, IgE is regulated by several cytokines as well as signaling receptors. Interleukin-4 (IL-4) activation of STAT6 promotes IgE class switching in B cells (Finkelman et al., 1988; Kopf et al., 1993; Shimoda et al., 1996). IL-21 is a potent suppressor of IgE responses, while CD40 signaling promotes

IgE (Yang et al., 2020). IgE has several unique features compared with other Ig isotypes including lower surface expression on B cells and increased differentiation of IgE+ B cells into plasma cells (Haniuda et al., 2016).

The germinal center (GC) micro-environment is required for antibody (Ab) affinity selection and high-affinity Ab production (Klein and Dalla-Favera, 2008; Victora and Nussenzweig, 2012), while high-affinity IgE is required for pathogenesis and anaphylaxis of allergic diseases (Gowthaman et al., 2019; Xiong et al., 2012). The GC is not a favorable environment for IgE+ B cells; IgE+ GC B cells have altered signaling, are more likely to undergo apoptosis, and are unlikely to develop into memory cells (Haniuda et al., 2016; Harris et al., 2005; He et al., 2013; Newman and Tolar, 2021; Saunders et al., 2019). It has been reported that low-affinity IgE is produced by IgE+ B cells through direct class switching, while indirect class switching from IgG1+ B cells accounts for high-affinity IgE (Erazo et al., 2007; He et al., 2017; Xiong et al., 2012; Yang et al., 2014). However, it is still controversial whether pathogenic high-affinity IgE can develop from IgE+ GC B cells (He et al., 2013; Talay et al., 2012; Yang et al., 2012). Overall, little is still known about the pathways regulating the initial class switching to IgE *in vivo* and expansion of IgE+ B cells in GC.

Several papers have suggested that the allergic response is dependent on T follicular helper (TFH) cells and that TFH-derived IL-4 is essential for the development of Ag-specific IgE (Ballesteros-Tato et al., 2016; Dolence et al., 2018; Kobayashi et al., 2017; Meli et al., 2017; Noble and Zhao, 2016; Zhang et al., 2020). Furthermore, a subset of TFH cells producing IL-13 (TFH13) is required for the development of high-affinity IgE (Gowthaman et al., 2019). T follicular regulatory (TFR) cells also regulate the development of IgE, either positively or negatively depending on the model used (Clement et al., 2019; Koh et al., 2020; Xie et al., 2020). Overall, much is still unknown about the precise role of TFH and TFR cells in allergen-specific IgE class switching and production.

In this study, we utilized an intragastric-sensitization food-allergy model and found that the timing of sensitization by the allergen is a critical factor for allergen-specific IgE production, which affects the expansion of Ag-specific B cells and the activity of TFH cells. In addition, we identified two molecules (fibrinogen-like protein 2 [*Fgl2*] and the ectonucleotidase CD39 [*Entpd1*]) produced by TFH cells that play an inhibitory role in regulating high-affinity IgE production.

## RESULTS

### Development of food-allergen-specific IgE requires two Ag sensitization steps

To better characterize the development of allergen-specific IgE in food allergy, we used a widely used method involving repeated intragastric priming or sensitization steps with peanut protein plus cholera toxin (PCT) (Li et al., 2000; Orgel and Kulis, 2018). Our first goal was to define the minimum sensitization steps required for the development of allergen-specific IgE (Figure 1A). We found that two PCT sensitization steps produced robust peanut (PN)-specific IgE and PN-specific IgG1 responses, while no PN-specific IgE or PN-specific IgG1 was detected following only one sensitization (Figure 1B). In contrast

to PN-specific IgE, total IgE is seen with just one sensitization (Figure 1B) and is higher after one PCT sensitization compared with naive mice (Figure 1C). In addition, the IgE produced by day 15 of this two-step sensitization model can cause anaphylaxis (Figure 1D). Thus, the development of allergen-specific IgE, but not total IgE, is dependent on a second sensitization step in this food-allergy model.

## The second sensitization step promotes the expansion of Ag-specific GC B cells and IgE+ GC B cells

To define exactly when allergen-specific IgE develops in the PCT food-allergy model, we measured the levels of IgE Abs at several time points before and after the second sensitization (Figure 2A). PN-specific IgE only emerged at day 12, 4 days after the second sensitization. PN-specific IgG1 could be detected at day 10 at a very low level. In contrast, total IgE could be detected at early as day 7 with titers increasing over the course of the experiment (Figures 1C and 2A). When ovalbumin (OVA) was used to replace PN, similar results were obtained in which OVA-specific IgE was first detected 4 days after the second sensitization (Figure S1A). These data indicate that Ag-specific IgE can develop early after the sensitization steps and likely does not require the formation of memory B cells. To characterize Ag-specific B cells in our model, an 4-hydroxy-3-nitrophenylacetyl (NP)-OVA hapten-protein conjugate was used in place of PN protein extract to allow for the detection of Ag-specific B cells (Figure S1B). Compared with naive mice, both the IgE+ GC B cells and NP-specific GC B cells increased significantly after the second sensitization (Figure 2B). Though at a very low level, NP-specific IgE+ GC B cells could be detected, and these cells increased significantly after the second sensitization (Figure 2B). IgE+ plasma cells and NP-specific IgE+ plasma cells also increased after the second sensitization (Figure S1C).

The IgG1+ B cell response showed similar kinetics to the IgE+ B cell response, with increases of IgG1+ GC B cells, NP-specific IgG1+ GC B cells, IgG1+ plasma cells, and NP-specific IgG1+ plasma cells after the second sensitization (Figures 2C and S1C). We hypothesized that the second sensitization may maintain the GC B cell response and inhibit apoptosis of GC B cells. We found that the percentage of both annexin V+ total GC B cells and annexin V+ IgE+ GC B cells decreased at least 2-fold after the second sensitization (Figure 2D). To better characterize the role of the second sensitization in the GC B cell response, we compared GC B cells and NP-specific GC B cells at day 12 following one or two sensitizations. We observed that, from day 8 to 12, NP-specific GC B cells decreased significantly without a second sensitization at day 8 (Figure 2E). The second sensitization rescued the NP-specific GC B cells and promoted the expansion of GC B cells and NP-specific GC B cells (Figure 2E). The expression of IgE germline transcript (ε GLT), a marker for IgE switching, mainly increased after the second sensitization, while the expression of GLT of IgG1 (γ1 GLT) and *Aicda* increased steadily (Figure S1D).

## Development of Ag-specific IgE, but not IgG1, is dependent on T cells and stimulation of Ag-specific B cells at second sensitization

Since the second sensitization is critical for the IgE response, we compared the role of Ag versus cholera toxin (CT) for the second sensitization. There was no significant difference

for the level of PN-specific IgE between groups in which PN or PN + CT were used at the second sensitization, while CT alone didn't induce PN-specific IgE at all (Figures 3A and S2A). These results suggest that the specific Ags are critical at the second sensitization. To determine whether the development of Ag-specific IgE is T helper cell dependent, we used NP-OVA, a T cell-dependent Ag, and NP-Ficoll, a T cell-independent Ag, in our food-allergy model. NP-specific IgE was detected in mice sensitized twice with NP-OVA but was absent in mice when NP-Ficoll was used (Figures 3B and S2B). In contrast, NP-specific IgG1 could be detected in all three groups (Figures 3B and S2B). This indicates that Ag-specific IgG1 can develop by a T cell-independent pathway. NP-specific GC B cell numbers were significantly lower when NP-Ficoll was used, suggesting that activation of T helper cells is critical to promote NP-specific GC B cells (Figure S2C). To study how B cells are involved in supporting Ag-specific IgE at second sensitization, we compared Ags only versus Ag-hapten conjugates (OVA versus NP-OVA) at the second sensitization after NP-OVA at the first sensitization. NP-IgE could only be produced with NP-OVA and not OVA alone, indicating that activation of existing NP-specific B cells at the second sensitization is critical (Figures 3C and S2D). To further study how T helper cells support Ag-specific IgE at the second sensitization, we used two different T cell Ags within the Ag-hapten conjugates (NP-OVA versus NP-KLH) at the second sensitization after NP-OVA sensitization at the first sensitization. NP-specific IgE was detected in mice receiving NP-OVA or NP-KLH sensitization at the second sensitization (Figures 3C and S2D). The similar level of NP-specific IgE regardless of the carrier protein used for the second sensitization indicates that the specificity of TFH cells is not critical at the second sensitization. At the same time, high levels of NP-specific IgG1 were produced in all conditions, again indicating a higher stringency in the development of Ag-specific IgE responses compared with Ag-specific IgG1 responses (Figure 3C).

To exclude that NP-KLH may be more potent than NP-OVA in inducing Ag-specific IgE, we compared different groups using a combination of NP-OVA and NP-KLH and found that there is no difference between these groups for the NP-specific IgE (Figure S2E). To study the effects on TFH cells when different combinations of Ags were used (Figure 3C), we characterized the level and activation status of TFH cells in GC (Figure S2F). We found that there were significantly more TFH cells, CD137-positive TFH cells, and CD90-negative/low TFH cells with NP-OVA at the second sensitization than the other Ags but not more CD69+ TFH cells (Figure S2G), suggesting that TFH cell activation and GC residency (Yeh et al., 2022) may be affected by the specific Ag presented by GC B cells. Overall, these data showed that the development of Ag-specific IgE in our food-allergy model is dependent on both T helper cell activation and the stimulation of existing Ag-specific B cells at the second sensitization. However, the specificity of T helper cells is not critical at the second sensitization for the development of Ag-specific IgE.

## Development of allergen-specific IgE, but not allergen-specific IgG1, requires proper timing of sensitization by allergen

The requirement of second sensitization in food allergy and the critical stimulation of Ag-specific B cells made us wonder whether the timing of the second sensitization could affect the development of Ag-specific IgE. We compared the PN-specific IgE and PN-

specific IgG1 in mice receiving their second sensitization at day 3, 8, or 15 after the first sensitization (Figure 4A).

Strikingly, the PN-specific IgE was only detectable in mice with sensitization at days 1 and 8, which contrasts with the development of PN-specific IgG1 that occurred following the secondary sensitization at all three time points (Figure 4A). The expression of ε-GLT and *Aicda,* but not γ1-GLT, were significantly higher in the days 1 and 8 group than the days 1 and 3 group (Figure 4B), further suggesting that Ag-specific IgE, but not IgG1, requires precise timing for the second sensitization in the food-allergy model. We measured the numbers of TFH, TFR, and GC B cells between days 1 and 3 and days 1 and 8 and didn't find any significant differences (Figures 4C and 4D), indicating a specific effect of timing on IgE regulation.

## Properly timed expansion of GC B cells is required for the development of Ag-specific IgE

We then investigated why the interval between the two sensitization steps affected the development of Ag-specific IgE. One hypothesis is that 3 days after the first sensitization, GC B cells cannot be activated at the second time, perhaps due to a refractory state from the first stimulation. Another hypothesis is that there are too few Ag-specific GC B cells at day 3 to stimulate with a second sensitization that will give a robust response. To test these hypotheses, mice were sensitized twice at days 1 and 8 then given a third sensitization at 3 days after the second sensitization (days 1, 8, and 11) or 7 days after the second sensitization (days 1, 8, and 15). Here, there is a large starting population of Ag-specific GCB to stimulate again, in contrast to the stimulation 3 days after just one sensitization. We observed that the titer of Ag-specific IgE with sensitization at days 1, 8, and 15 was significantly higher than the days 1, 8, and 11 titer (Figure 5A). To exclude the possibility that the difference observed is caused by the prolonged interval between analysis and last sensitization, we measured PN-specific IgE at similar days after the last sensitization, and the PN-specific IgE was still significantly higher with sensitization at days 1, 8, and 15 than at days 1, 8, and 11 (Figure 5B). NP-specific GC B cell numbers were not significantly affected by the differently timed sensitizations (Figure 5C). These data suggested that an Ag-specific IgE response requires an optimal period of time between sensitizations, past an initial refractory period where GCB cells cannot be productively stimulated again. This refractory period appears to particularly critical for IgE+ GC B cells. To understand why a longer time between sensitizations doesn't lead to an IgE response, we measured GC B cell numbers over time after one sensitization. GC B cell and Ag-specific GC B cell numbers were higher at day 8 than that at days 3 and 15 (Figure 5D), indicating that these cells decay after the day 8 peak. Additionally, IgG1+ GC B cells and CD138+ plasma cells were consistent with a cellular response that is highest at day 8 (Figure S3A). These results suggested that the optimal expansion of GC B cells relies on the second sensitization of Ag-specific GC B cells at day 8, which leads to the development of Ag-specific IgE in the food-allergy model. However, the apoptosis of GC B cells was not significantly affected by different timings of sensitizations (Figure S3B). Taking these data together, we can construct a model where an early second sensitization cannot stimulate Ag-specific GC B cells to produce an Ag-specific IgE response, whereas too late of a second sensitization leads to

apoptotic loss of the Ag-specific GC B cells before they can generate an Ag-specific IgE response.

### TFH and TFR gene expression is altered by timing of Ag sensitization

In Figure 3, we show that the development of Ag-specific IgE is T cell-dependent at both sensitization steps, and our earlier studies showed that both TFH and TFR cells are required for IgE production (Xie et al., 2020). We then wondered if the sensitization timing affected the nature of the help from TFH cells and also the suppression capacity of TFR cells. We therefore used RNA sequencing (RNA-seq) to profile gene expression of TFH and TFR cells from mice sensitized at days 1 and 3 and days 1 and 8 (Table S1). In TFH cells, the expression of 1,483 out of 12,275 genes increased by at least 1.5-fold, while the expression of 1,787 genes out of 12,275 genes decreased by at least 1.5-fold in the days and 8 group compared with the days 1 and 3 group. In TFR cells, 1,263 genes out of 12,162 genes increased expression by at least 1.5-fold, while 3,213 genes out of 12,162 genes decreased in expression by at least 1.5-fold in the days 1 and 8 group compared with the days 1 and 3 group. We focused specifically on the known regulatory factors expressed by TFH and TFR cells that might regulate IgE switching and the survival and proliferation of IgE+ GC B cells. The expression of the majority of genes that play important roles in the function of TFH and TFR cells (signaling receptors *Cxcr5, Cd40lg, Icos, Pdcd1*; cytokines *Il4, Il10, Il21, Tgfb1, Ifng*; cytokine receptors *Il1r2, Il1rn, Il2ra*; inhibitory molecules *Tigit, Fasl, Tnfsf10, Lag3, Ctla4, Gzmb*) were unchanged between TFH and TFR cells from mice sensitized on days 1 and 3 and days 1 and 8 (Figures 6A-6C, S4A, and S4B). Analysis of IL-4-producing TFH cells using *Il4* reporter mice (4get) showed separately that there is no difference in TFH-derived IL-4 between sensitizations at days 1 and 3 and days 1 and 8 (Figure S4C). It has been reported that TFR cells produce the inhibitory factor Neuritin (*Nrn1*) to repress IgE (Gonzalez-Figueroa et al., 2021). In our food-allergy model, we observed a 2-fold decrease in *Nrn1* in TFR cells after sensitization at days 1 and 8 compared with at days 1 and 3 (Figures 6A-6C and S4D). Unexpectedly, we also observed a 2-fold decrease in *Nrn1* in TFH cells after sensitization at days 1 and 8 compared with at days 1 and 3 (Figures 6A-6C and S4D). We therefore examined both TFH and TFR cells for changes in the expression of other suppressor genes. *Fgl2* and *Entpd1* are immune-suppressive factors typically associated with Tregs, but their function in regulating Ab production has not been extensively studied (Liu et al., 2017; Shalev et al., 2008; Wang et al., 2015). We observed that *Fgl2* and *Entpd1* had a marked decrease in expression in days 1 and 8 TFH cells compared with days 1 and 3 TFH cells (Figures 6A-6C). *Fgl2* showed a 13.6-fold decrease in TFH cells and a 5.5-fold decrease in TFR cells from days 1 and 3 to days 1 and 8. (Figures 6A-6C). Independent qPCR data validated that the expression of *Fgl2* and *Entpd1* in TFH cells was significantly lower in the days 1 and 8 group than the days 1 and 3 group (Figure 6B). While the expression of *Fgl2* was significantly lower in TFR cells from the days 1 and 8 group, *Entpd1* was not significantly altered in TFR cells (Figures 6C and 6D). As expected, both *Fgl2* and *Entpd1* were more highly expressed in TFR cells compared to TFH cells (Figure 6E). Overall, the expression pattern we observed for *Fgl2* and *Entpd1* implied that they may play a suppressive role in regulating Ag-specific IgE in this food-allergy model.

### CD39 and TFH-derived FGL2 inhibit Ag-specific IgE

We then tested whether the expression of *Entpd1* was affected by the second sensitization. qRT-PCR data showed that *Entpd1* gene expression is significantly down-regulated after the second sensitization in TFH cells but not in TFR cells (Figure S5A). To test whether CD39 regulates the development of Ag-specific IgE in our food-allergy model, a specific CD39 inhibitor (POM-1) was used. Flow cytometry showed that POM-1 treatment increased the percent of IgE+ GC B cells compared with control mice (Figure S5B), and we found that after PCT sensitization at days 1 and 8, POM-1 treatment led to slightly more PN-specific IgE (Figure S5C). PN-specific IgG1 was not different between control and POM-1-treated mice (Figure S5C).

We next tested whether the expression of *Fgl2* was affected by the second sensitization. qRT-PCR data showed that *Fgl2* gene expression is significantly down-regulated after the second sensitization in TFH cells but not in TFR cells (Figure 7A). To further investigate the role of *Fgl2* in the development of Ag-specific IgE in our food-allergy model, we initially tested *Fgl2* germline knockout (−/−) mice. *Fgl2*$^{-/-}$ mice showed higher titers of PN-specific IgE than wild-type (WT) mice but unchanged titers of PN-specific IgG1 (Figure 7B). *Fgl2*$^{-/-}$ mice also showed more TFH cells and GC B cells, but not TFR cells, than WT mice (Figure S6A). *Fgl2*$^{-/-}$ mice also showed decreased apoptosis of GC B cells than WT mice (Figure S6B). To see whether the deletion of *Fgl2* and inhibition of CD39 could rescue IgE in timed sensitizations at days 1 and 3, we compared PN-specific IgE in WT mice, *Flg2*$^{-/-}$ mice, and *Fgl2*$^{-/-}$ with POM-1 treatment in mice that were sensitized with PCT at days 1 and 3. It was found that PN-specific IgE significantly increased in *Fgl2*$^{-/-}$ mice treated with POM-1 (Figure 7C), suggesting that combined *Fgl2* deletion and CD39 inhibition partly reversed the Ag-specific IgE deficiency with sensitizations at days 1 and 3. A bone marrow (BM) chimera experiment was then designed to compare the role of Fgl2 from TFH cells and TFR cells versus Fgl2 from TFR cells alone. BM chimeras with *Fgl2*$^{-/-}$ BM plus Cd4-Cre Bcl6-flox BM allowed us to test the effect of loss of *Fgl2* in both TFH and TFR cells, whereas BM chimeras with *Fgl2*$^{-/-}$ BM plus Foxp3-Cre Bcl6-flox BM allowed us to test the effect of loss of *Fgl2* in TFR cells alone (Figure 7D). We found that mice with *Fgl2*-deficient TFH and TFR cells developed higher PN-specific IgE than control mice or mice with *Fgl2*-deficient TFR cells (Figure 7E). Ag-specific IgG1 and total IgE was also higher in mice with *Fgl2*-deficient TFH and TFR cells than in mice with *Fgl2*-deficient TFR cells (Figure S6C). These data imply that *Fgl2* expressed by TFH cells is negatively regulating Ag-specific IgE. To study whether the pathogenic function of IgE was affected by *Fgl2* deficiency in TFH cells, we tested the anaphylactic response in the BM chimeric mice. We found that anaphylaxis is much more severe, measured by temperature drop, in mice with *Fgl2*-deficient TFH and TFR cells than in control mice and mice with *Fgl2*-deficient TFR cells alone (Figure 7F). GC B cells were also higher in mice with *Fgl2*-deficient TFH and TFR cells than control mice or mice with *Fgl2*-deficient TFR cells alone (Figure 7G). Thus, FGL2 derived from TFH cells regulates the production of anaphylactic IgE in this food-allergy model. These data show that a regulatory factor expressed by TFH cells can specifically repress Ag-specific IgE production and that the expression of these factors is regulated by the timing of allergen sensitization steps.

## DISCUSSION

Here, we used a food-allergy model in mice to reveal several aspects of how Ag-specific IgE responses develop within the GC reaction and are regulated by TFH cells. We found that both the timing of allergen sensitization and the specific form of the Ag required to stimulate GC B cells were critical for the development of Ag-specific IgE but not for Ag-specific IgG1. The allergen-sensitization timing affects the expansion of Ag-specific GC B cells and affects the nature of the help from TFH cells. We further discovered that two genes, *Fgl2* and *Entpd1*, which are regulated by the timing of allergen sensitization, play inhibitory roles in the development of Ag-specific IgE. Finally, we found that expression of *Fgl2* specifically from TFH cells suppresses the Ag-specific IgE response and anaphylaxis.

Though IgE responses have been studied for decades, details about how the Ag-specific IgE response is initiated *in vivo*, particularly in GC, remains unknown. It is still not fully understood at what stage IgE class switching of Ag-specific B cells occurs *in vivo* and the complete sequence of signals involved (Satitsuksanoa et al., 2021). Here, we have described a detailed pathway for allergen-specific IgE production where a minimum of two allergen sensitization steps are required, in a very specific time frame. We showed that the two sensitization steps are necessary to expand significant numbers of Ag-specific GC B cells, including IgE+ Ag-specific GC B cells. Ig switching to IgE in GC occurs at a low level compared with switching to IgG1, which reflects the fact that IgE class switching is tightly controlled (Newman and Tolar, 2021; Wade-Vallance and Allen, 2021). One model for high-affinity IgE responses is that there is competition between IgG1 and IgE class switching by B cells within the GC. IgE promoting signals such as IL-4 are limiting factors, while IL-21 inhibits IgE switching (Wesemann et al., 2011; Wu et al., 2017; Yang et al., 2020). Our data support the model that the GC reaction plays a critical role in the development of Ag-specific IgE and that repeated sensitization promotes more IgE production in the GC. The consensus in the IgE field is that IgE+ B cells are not efficiently expanded and selected in the GC and thus do not generate high-affinity IgE production. In this model, high-affinity IgE is typically produced through sequential switching from IgG1+ B cells that have previously gone through affinity selection in the GC (Gould and Ramadani, 2015; He et al., 2015; Turqueti-Neves et al., 2015). The stage at which IgG1+ B cells switch to IgE is not well characterized, but some studies indicate that this occurs at a memory B cell stage (Jimenez-Saiz et al., 2018, 2019). Our findings with this food-allergy model do not fit with sequential switching to IgE from IgG1+ memory B cells, since a 7 day spacing in sensitization produced Ag-specific IgE, but a 15 day spacing did not produce Ag-specific IgE. If memory B cells were involved, the 15 day spacing should have worked as well or better to produce IgE than the 7 day spacing. Thus, our data suggest that Ag-specific IgE develops specifically within the GC in the food-allergy model. In addition, we found that Ag-specific IgE emerged as early as day 12, which is only 2 days after the Ag-specific IgG1, suggesting that IgE and IgG1 response develop nearly simultaneously within the GC. We have also found in this food-allergy model that high-affinity IgE, which can promote anaphylaxis, is produced as early as day 15 (Figure 1D). Whether sequential class switching of IgE through an IgG1 intermediate can occur efficiently within this time frame is not clear.

We are currently studying whether high-affinity IgE can develop by direct switching in the GC or whether sequential class switching from IgG1 to IgE occurs within the GC.

One oddity we observed is the increase in total IgE level after just one sensitization, while ε GLT expression only increases after two sensitizations. Possible reasons for the discrepancy are that either the signal to induce the ε GLT is stronger at day 12 than day 8 and/or that an increase of IgE+ plasma cells giving rise to increased serum IgE is not captured in the total B cell population analyzed.

While we have increased our understanding of the role of the second allergen sensitization step in inducing IgE responses, some questions remain. We showed that CT is not required at the second sensitization, suggesting that tolerance is broken at the first sensitization and that only Ag is needed to stimulate B and T cells at the second sensitization. Unexpectedly, using B cell haptens coupled to different T cell Ags, we found that TFH cells at the second sensitization do not require the same Ag used in the first sensitization to help Ag-specific B cells. However, for both sensitization steps, the cognate B cell Ag needs to be linked to the cognate T cell Ag. The most likely explanation for these results is that newly generated TFH cells can enter pre-existing GCs to provide help to IgE+ B cells after the second sensitization. Previous work showed that newly generated TFH cells could seed ongoing GCs and provide help (Shulman et al., 2013), but here we show that this can occur in the context of an IgE response. A second explanation is that rather than newly generated TFH cells entering the GC, non-Ag-specific bystander TFH cells outside the GC can provide help to B cells if given the proper Ag stimulation (Ritvo et al., 2018; Wan et al., 2019). Future work is needed to understand if the help to IgE+ GC B cells is delivered by cognate TFH cells or from bystander TFH cells.

Another striking finding from our study is the differential regulation of Ag-specific IgE and Ag-specific IgG1. We observed that Ag-specific IgG1 is not sensitive to the timing of sensitization steps, unlike IgE. It has been reported that Ag-specific IgE, but not IgG1, is extremely sensitive to IL-4 levels (Robinson et al., 2017). Ag-specific IgE+ GC B cells may also be more sensitive to the levels of both positive and negative regulatory factors than IgG1. This hypothesis is consistent with our data showing that Ag-specific IgE, but not IgG1, is affected in *Fgl2*-deficient mice and CD39 inhibitor treatment. Additionally, Ag-specific IgE, but not IgG1, requires stimulation of pre-existing GC B cells at the second sensitization. Several papers have shown that IgE+ GC B cells display distinct features from IgG1+ GC B cells, including less surface immunoglobin receptor expression and greater propensity to undergo apoptosis or differentiate into short-lived plasma cells (Haniuda et al., 2016). The differential survival and differentiation capabilities of switched IgE+ GC B cells and IgG1+ GC B cells may contribute to different outcomes of Ag-specific IgE and IgG1 in our food-allergy model.

Several papers have shown that the Ag-specific IgE response is dependent on TFH and TFR cells (Ballesteros-Tato et al., 2016; Clement et al., 2019; Kobayashi et al., 2017; Noble and Zhao, 2016). The mechanism for how TFH and TFR cells regulate the IgE response is just starting to be understood and includes the IL-4, IL-13, IL-10, IL-21, and IL-2 signaling pathways (Dolence et al., 2018; Gowthaman et al., 2019; Meli et al., 2017; Xie

et al., 2020; Yang et al., 2020). New molecules have recently been discovered that regulate the GC and IgE response. TFR cells produce the inhibitory factor *Nrn1* to regulate IgE (Gonzalez-Figueroa et al., 2021). Interestingly, we also observed lower expression of *Nrn1* in TFH and TFR cells after sensitization at days 1 and 8 compared with at days 1 and 3, supporting an inhibitory role of *Nrn1* in regulating IgE. Here, we have identified two factors with differential expression between PCT sensitization at days 1 and 3 and days 1 and 8, Fgl2 and CD39, and their roles in regulating Ag-specific IgE were characterized. Previous work on the immunoregulatory role of Fgl2 has focused on its role in regulatory T cells (Tregs) and suppressing immune responses (Liu et al., 2017; Shalev et al., 2008; Wang et al., 2015). Most recently, Fgl2-derived from TFR cells was found to regulate the Ab response (Sungnak et al., 2020). Interestingly, these researchers found that the expression of *Fgl2* is not detectable in TFH cells but is quite high in TFR cells (Sungnak et al., 2020). We have analyzed the GC and Ag-specific IgE response in *Fgl2*-deficient mice and conclude that TFH cell-derived, instead of TFR cell-derived, Fgl2 inhibits Ag-specific IgE production and the anaphylactic reaction in our food-allergy model. Unlike Ag-specific IgE, Ag-specific IgG1 was not affected by *Fgl2* deficiency in mice in our food-allergy model. Whether Fgl2 regulates the GC response generally and affects IgE+ B cells more intensely, as these cells are more sensitive to regulatory signals, or whether Fgl2 more specifically regulates IgE+ GC B cells, needs future study. We note that the expression of *Fgl2* and *Entpd1* were also higher in TFH cells with an aberrant granzyme B+ phenotype, which correlated with poor Ag-specific IgE production (Xie et al., 2019). These data further suggest an inhibitory role of *Fgl2* and *Entpd1* in TFH cells. However, since we used a pharmaceutical CD39 inhibitor, we were unable to study the role of CD39 specifically in TFH or TFR cells. A mouse model with a specific deletion of *Entpd1* or *Fgl2* in TFH cells is not currently available. The key question of how the expression of *Fgl2, Entpd1,* and other inhibitory factors are regulated in TFH cells during the IgE response needs more investigation.

In this study, we observed that the timing of allergen sensitization determined whether specific IgE was produced or not, with too short of a window or too long of a window between allergen sensitizations leading to a failed IgE response. We showed that a short period of timing between allergen sensitization steps blocked development of IgE+ B cells and relates in part to expression of inhibitory factors, such as *Fgl2* and *Entpd1*, by TFH cells. Whether human food allergy depends on a similar pattern of exposure to allergens is not clear. Overall, this study adds important details to our knowledge of how Ag-specific IgE responses are regulated in the development of food allergy, which may inform the human IgE response.

## Limitations of the study

This study focused on how high-affinity IgE responses develop after gut sensitization using protein Ags plus CT as an adjuvant. This system is a widely used mouse model for food allergy but differs from the development of food allergy in humans, which is not associated with CT. We showed that in the optimal sensitization sequence for strong IgE responses, the immune-suppressive genes Fgl2 and Entpd1 are down-regulated in TFH cells. However, these are only a subset of genes and factors altered by the timing of Ag sensitization, and we have not characterized all factors regulated by the timing of Ag sensitization. We

observed that genetic ablation of *Fgl2* in both TFH and TFR cells, but not in TFR cells alone, increased Ag-specific IgE levels and IgE-mediated anaphylactic responses. Since we are unable to delete genes specifically in TFH cells without affecting TFR cells, we cannot rule out that TFR cells produce Fgl2 that influences IgE responses; however, loss of Fgl2 by TFR cells alone is not sufficient to significantly affect IgE responses. Furthermore, we do not have a genetic model to delete *Entpd1* in TFH and TFR cells and had to rely on an inhibitor compound that may affect other cell types. Additionally, we do not know how applicable our results are to other model systems where IgE responses are induced. Finally, we do not yet know how our results relate to the human IgE response.

## STAR★METHODS

### RESOURCE AVAILABILITY

**Lead contact—**Further information and requests for resource/reagents should be directed to and will be fulfilled by the lead contact, Alexander Dent (adent2@iupui.edu).

**Materials availability—**This study did not generate new unique reagents.

**Data and code availability—**Data availability. The RNA-seq datasets generated in this paper are available at the NCBI GEO database (GEO: GSE202713).

Code availability. This paper does not report original code.

Any additional information required to reanalyze the data reported in this paper is available from the lead contact upon request.

### EXPERIMENTAL MODEL AND SUBJECT DETAILS

**Mouse strains—**All mutant mice were on a C57BL/6 background. Foxp3-Cre Bcl6-flox (Bcl6FC), and Cd4-Cre Bcl6-flox (Bcl6 cKO) mice were described previously (Hollister et al., 2013; Wu et al., 2016). C.129-*Il4*$^{tm1Lky/J}$ (4get) were obtained from The Jackson Laboratory. IgE reporter mice *Igh*-7$^{tm1.2Cdca}$ (Verigem) were obtained from Dr. Chris Allen (UCSF) (Yang et al., 2012). *Fgl2* knockout (*Fgl2* −/−) mice were obtained from Dr. Gary A. Levy (University of Toronto) (Marsden et al., 2003). Six-to ten-week-old male and female mice were used for most experiments. Mouse littermate comparisons were used whenever possible. Control and experimental mouse cohorts were age and sex matched. Mice were bred under specific pathogen–free conditions at the laboratory animal facility of the Indiana University School of Medicine. All experiments and handling of animals were conducted according to protocols approved by the IACUC of the Indiana University School of Medicine.

### METHOD DETAILS

**Gut sensitization—**Mice were deprived of food for 2 h, and then each mouse was fed 300 μL 1.5% $NaHCO_3$ water (i.g.). Thirty minutes later, each mouse was given 1 mg peanut protein extract (Greer Laboratories), OVA (Sigma), KLH (Sigma), $NP_{16}$-OVA (Biosearch), or $NP_{18}$-KLH (Biosearch) together with 10 μg cholera toxin (Sigma) according to the setting of experiments (Li et al., 2000; Orgel and Kulis, 2018). The mice were sacrificed on the

indicated days and the mesenteric lymph nodes (mLN) and spleen were harvested. Serum was collected.

**Assessment of anaphylaxis—**To assess anaphylaxis, 2 mg peanut (PN) without cholera toxin (CT) was injected i.p. per mouse at the indicated time points after sensitization. Mice were monitored for 40 min after challenge for the rectal (core) body temperature (Braintree Scientific).

**Total B cell isolation—**Total cells were harvested from mLN and spleen. B cells were isolated using B Cell Isolation Kit, mouse (Miltenyi) according to manufacturer's instruction.

**ELISA—**For the measurement of PN-specific IgE, 96 well Nunc-Immuno plates (Sigma) were coated with 5 μg/mL IgE Ab (Clone: LO-ME-3, BIO-RAD) in 0.1 M Carbonate buffer (pH 9.5) overnight at 4°C. Wells were blocked with 1% BSA for at least 1 h at room temperature and diluted serum was added and incubated at room temperature for 2 h. Peanut protein extract was labeled with biotin (Sigma) and added into wells for one hour (2 μg/mL) followed by adding poly-HRP streptavidin (Pierce Endogen) for 0.5 h (1:2000). For PN-specific IgG1, 96 well Nunc-Immuno plates were coated with 5 ug/mL peanut protein extract in 0.1 M Carbonate buffer (pH 9.5) overnight at 4°C. Wells were blocked with 1% BSA for at least 1 h at room temperature and diluted serum was added and incubated at room temperature for 2 h. An anti-mouse IgG1 (Clone: A85-1, BD Pharmingen) was used as secondary Ab (2 μg/mL) followed by adding avidin-HRP (Invitrogen) for 0.5 h (1:2000). For total IgE, 96 well Nunc-Immuno plates were coated with 2 ug/mL anti-mouse IgE (Clone: R35-72, BD Pharmingen) overnight at 4°C. Wells were blocked with 1% BSA for at least 1 h at room temperature and diluted serum was added and incubated at room temperature for 2 h. An anti-mouse IgE (Clone: R35-118, BD Pharmingen) was used as secondary Ab (2 μg/mL) followed by adding avidin-HRP (Invitrogen) for 0.5 h (1:2000). After the incubation with HRP, TMB Substrate Reagent Set (BD Pharmingen) was added for the reaction development.

**Flow cytometry—**Cell suspensions from mLNs were prepared and filtered through a 40-μm cell strainer (Fisherbrand). Cells were washed and diluted in PBS with 1% FBS and were stained with Fc block (Biolegend) for 5 min, followed by surface staining for the indicated markers. Following labeled Abs were used: anti-CXCR5 (L138D7), anti-PD-1 (29F.1A12), anti-CD4 (RM4-5), anti-CD38 (90) and anti-B220 (RA3-6B2), anti-GL7 (GL7), anti-IgG1 (RMG1-1), anti-Foxp3 (MF-14) were obtained from BioLegend. For Annexin V staining, PE Annexin V (BioLegend) was added after surface staining using Annexin V binding buffer (BioLegend) according to the instruction. For NP-specific B cells staining, $NP_{16}$-PE was added at the concentration of 5 nM and incubated on ice for 30 min. Fixation/ Permeablization Kit (BD Pharmingen) was used for intracellular staining following surface staining. All samples were acquired on an LSR2 flow cytometer (Becton Dickinson) and analyzed with FlowJo V10.6 (TreeStar).

**Q-PCR—**The mRNA expression of cytokines, *Fgl2,* and *Entpd1* were measured using Taqman Fast Advanced Master Mix (Thermo Fisher) in QuantStudio 6

and 7 Flex Real-Time PCR System (Thermo Fisher). The probes for *Il4* (Mm00445259), *Il21* (Mm00517640), *Il10* (Mm00439614), *Ifng* (Mm01168134), *Cd40lg* (Mm00441911), *Fgl2* (Mm00433327), *Entpd1* (Mm00515448), *Tubb5* (Mm00495806), *Aicda* (Mm01184115) were purchased from Thermo Fisher. Taqman probes for γ1-GLT (Probe: 5′-FAM-TGGTTCTCTCAACCTGTAGTC CATGCCA-3', Forward: 5′-CGAGAAGCCTGAGGAATGTGT-3′, Reverse: 5′-GGAGTTAGTTTGGGCAGCAGAT-3') and ε-GLT (Probe: 5′-FAM-CAGCCACTCACTTATCAGAG-3′, Forward: 5′-GCAGAAGATGGCTTCGAATAAGAACAGT-3', Reverse: 5′-TCGTTGAATGATGGAGGATGTGTCACGT-3′) were purchased from Custom TaqMan Probes (Roco et al., 2019).

**Bone marrow chimera—**Bone marrow cells ($2.5 \times 10^6$ each type) from donor mice were mixed and then injected i.v. into *Rag1* −/− recipient mice which were sublethally irradiated (350 Gy). The lymphoid compartment in the recipients was allowed to constitute for 2 months before PCT sensitization.

## QUANTIFICATION AND STATISTICAL ANALYSIS

**RNA-seq and analysis—**RNA-seq was performed by the Indiana University School of Medicine Center for Medical Genomics. Uniquely mapped sequencing reads were assigned to mm10 refGene genes. Quality control of sequencing and mapping results was summarized using MultiQC. Genes with read count per million (CPM) < 0.5 in more than 4 of the samples were removed. The data was normalized using TMM (trimmed mean of M values) method. Differential expression analysis was performed using edgeR. False discovery rate (FDR) was computed from p values using the Benjamini-Hochberg procedure. Differentially expressed genes (DEGs) were determined if their p-values were less than 0.05 after multiple-test correction with FDR-adjustment and the amplitude of fold changes (FCs) were larger than 1.8. The RNA-seq data can be accessed via NCBI GEO database (GEO: GSE202713).

**Statistical analysis—**All data analysis was performed using GraphPad Prism software (GraphPad Software). Graphs show the mean ± SEM. Unless otherwise stated, Two-tailed Student's t test or One-way ANOVA with Tukey's post hoc analysis was used. All ELISAs were analyzed using two-way ANOVA with Holm-Šidák multiple comparisons test. Significant differences ($p < .05$) and some non-significant differences are indicated in the figures. All the statistical details of experiments can be found in figure legends. The investigators were not blinded for the analyses.

## Supplementary Material

Refer to Web version on PubMed Central for supplementary material.

## ACKNOWLEDGMENTS

We would like to thank Dr. Chris Allen (UCSF) for the kind gift of the Verigem IgE reporter mice and Dr. Gary A. Levy (University of Toronto) for the kind gift of the *Fgl2* knockout (*Fgl2*$^{-/-}$) mice. We would like to thank Caleb Corn for help with mouse genotyping and Drs. Baohua Zhou and Mark Kaplan for critical evaluation of the manuscript. We thank Tony Sinn for assistance with mouse irradiation and BM transplantation. This work was

supported by Public Health Service grants from the National Institutes of Health (grant R01 AI132771 to A.L.D.). Core facility use (flow cytometry and mouse manipulation) was also supported by Indiana University Simon Cancer Center Support Grants (P30 CA082709 and U54 DK106846).

## REFERENCES

Asher MI, Montefort S, Björkstén B, Lai CK, Strachan DP, Weiland SK, Williams H, and Group, I.P.T.S. (2006). Worldwide time trends in the prevalence of symptoms of asthma, allergic rhinoconjunctivitis, and eczema in childhood: ISAAC Phases One and Three repeat multicountry cross-sectional surveys. Lancet 368, 733–743. 10.1016/S0140-6736(06)69283-0. [PubMed: 16935684]

Ballesteros-Tato A, Randall TD, Lund FE, Spolski R, Leonard WJ, and Leon B (2016). T follicular helper cell plasticity shapes pathogenic T helper 2 cell-mediated immunity to inhaled house dust mite. Immunity 44, 259–273. 10.1016/j.immuni.2015.11.017. [PubMed: 26825674]

Clement RL, Daccache J, Mohammed MT, Diallo A, Blazar BR, Kuchroo VK, Lovitch SB, Sharpe AH, and Sage PT (2019). Follicular regulatory T cells control humoral and allergic immunity by restraining early B cell responses. Nat. Immunol 20, 1360–1371. 10.1038/s41590-019-0472-4. [PubMed: 31477921]

Dolence JJ, Kobayashi T, Iijima K, Krempski J, Drake LY, Dent AL, and Kita H (2018). Airway exposure initiates peanut allergy by involving the IL-1 pathway and T follicular helper cells in mice. J. Allergy Clin. Immunol 142, 1144–1158.e8. 10.1016/j.jaci.2017.11.020. [PubMed: 29247716]

Erazo A, Kutchukhidze N, Leung M, Christ APG, Urban JF Jr., Curotto de Lafaille MA, and Lafaille JJ (2007). Unique maturation program of the IgE response in vivo. Immunity 26, 191–203. 10.1016/j.immuni.2006.12.006. [PubMed: 17292640]

Finkelman FD, Katona IM, Urban JF, Holmes J, Ohara J, Tung AS, Sample JV, and Paul WE (1988). IL-4 is required to generate and sustain in vivo IgE responses. J. Immunol 141, 2335–2341. [PubMed: 2459206]

Gonzalez-Figueroa P, Roco JA, Papa I, Núñez Villacís L, Stanley M, Linterman MA, Dent A, Canete PF, and Vinuesa CG (2021). Follicular regulatory T cells produce neuritin to regulate B cells. Cell 184, 1775–1789.e19. 10.1016/j.cell.2021.02.027. [PubMed: 33711260]

Gould HJ, and Ramadani F (2015). IgE responses in mouse and man and the persistence of IgE memory. Trends Immunol. 36, 40–48. 10.1016/j.it.2014.11.002. [PubMed: 25499855]

Gould HJ, and Ramadani F (2018). Peanut allergen-specific antibodies go public. Science 362, 1247–1248. 10.1126/science.aav3709. [PubMed: 30545875]

Gould HJ, Sutton BJ, Beavil AJ, Beavil RL, McCloskey N, Coker HA, Fear D, and Smurthwaite L (2003). The biology of IgE and the basis of allergic disease. Annu. Rev. Immunol 21, 579–628. 10.1146/annurev.immunol.21.120601.141103. [PubMed: 12500981]

Gowthaman U, Chen JS, Zhang B, Flynn WF, Lu Y, Song W, Joseph J, Gertie JA, Xu L, Collet MA, et al. (2019). Identification of a T follicular helper cell subset that drives anaphylactic IgE. Science 365, eaaw6433. 10.1126/science.aaw6433. [PubMed: 31371561]

Haniuda K, Fukao S, Kodama T, Hasegawa H, and Kitamura D (2016). Autonomous membrane IgE signaling prevents IgE-memory formation. Nat. Immunol 17, 1109–1117. 10.1038/ni.3508. [PubMed: 27428827]

Harris MB, Mostecki J, and Rothman PB (2005). Repression of an interleukin-4-responsive promoter requires cooperative BCL-6 function. J. Biol. Chem 280, 13114–13121.10.1074/jbc.M412649200. [PubMed: 15659391]

He J-S, Narayanan S, Subramaniam S, Ho WQ, Lafaille JJ, and Curotto de Lafaille MA (2015). Biology of IgE production: IgE cell differentiation and the memory of IgE responses. In IgE Antibodies: Generation and Function, Lafaille JJ and Curotto de Lafaille MA, eds. (Springer International Publishing), pp. 1–19.

He JS, Meyer-Hermann M, Xiangying D, Zuan LY, Jones LA, Ramakrishna L, de Vries VC, Dolpady J, Aina H, Joseph S, et al. (2013). The distinctive germinal center phase of IgE+ B lymphocytes limits their contribution to the classical memory response. J. Exp. Med 210, 2755–2771.10.1084/jem.20131539. [PubMed: 24218137]

He JS, Subramaniam S, Narang V, Srinivasan K, Saunders SP, Carbajo D, Wen-Shan T, Hidayah Hamadee N, Lum J, Lee A, et al. (2017). IgG1 memory B cells keep the memory of IgE responses. Nat. Commun 8, 641. 10.1038/s41467-017-00723-0. [PubMed: 28935935]

Hollister K, Kusam S, Wu H, Clegg N, Mondal A, Sawant DV, and Dent AL (2013). Insights into the role of Bcl6 in follicular Th cells using a new conditional mutant mouse model. J. Immunol 191, 3705–3711. 10.4049/jimmunol.1300378. [PubMed: 23980208]

Jiménez-Saiz R, Bruton K, Koenig JFE, Waserman S, and Jordana M (2018). The IgE memory reservoir in food allergy. J. Allergy Clin. Immunol 142, 1441–1443. 10.1016/j.jaci.2018.08.029. [PubMed: 30201515]

Jiménez-Saiz R, Ellenbogen Y, Koenig JFE, Gordon ME, Walker TD, Rosace D, Spill P, Bruton K, Kong J, Monteiro K, et al. (2019). IgG1+ B-cell immunity predates IgE responses in epicutaneous sensitization to foods. Allergy 74, 165–175. 10.1111/all.13481. [PubMed: 29790165]

Klein U, and Dalla-Favera R (2008). Germinal centres: role in B-cell physiology and malignancy. Nat. Rev. Immunol 8, 22–33. 10.1038/nri2217. [PubMed: 18097447]

Kobayashi T, Iijima K, Dent AL, and Kita H (2017). Follicular helper T cells mediate IgE antibody response to airborne allergens. J. Allergy Clin. Immunol 139, 300–313.e7. 10.1016/j.jaci.2016.04.021. [PubMed: 27325434]

Koh B, Ulrich BJ, Nelson AS, Panangipalli G, Kharwadkar R, Wu W, Xie MM, Fu Y, Turner MJ, Paczesny S, et al. (2020). Bcl6 and Blimp1 reciprocally regulate $ST2^+$ Treg–cell development in the context of allergic airway inflammation. J. Allergy Clin. Immunol 146, 1121–1136.e9. 10.1016/j.jaci.2020.03.002. [PubMed: 32179158]

Kopf M, Gros GL, Bachmann M, Lamers MC, Bluethmann H, and Köhler G (1993). Disruption of the murine IL-4 gene blocks Th2 cytokine responses. Nature 362, 245–248. 10.1038/362245a0. [PubMed: 8384701]

Li XM, Serebrisky D, Lee SY, Huang CK, Bardina L, Schofield BH, Stanley JS, Burks AW, Bannon GA, and Sampson HA (2000). A murine model of peanut anaphylaxis: T- and B-cell responses to a major peanut allergen mimic human responses. J. Allergy Clin. Immunol 106, 150–158. 10.1067/mai.2000.107395. [PubMed: 10887318]

Liu XG, Liu Y, and Chen F (2017). Soluble fibrinogen like protein 2 (sFGL2), the novel effector molecule for immunoregulation. Oncotarget 8, 3711–3723. 10.18632/oncotarget.12533. [PubMed: 27732962]

Marsden PA, Ning Q, Fung LS, Luo X, Chen Y, Mendicino M, Ghanekar A, Scott JA, Miller T, Chan CW, et al. (2003). The Fgl2/fibroleukin prothrombinase contributes to immunologically mediated thrombosis in experimental and human viral hepatitis. J. Clin. Invest 112, 58–66. 10.1172/JCI18114. [PubMed: 12840059]

Meli AP, Fontés G, Leung Soo C, and King IL (2017). T follicular helper cell-derived IL-4 is required for IgE production during intestinal helminth infection. J. Immunol 199, 244–252. 10.4049/jimmunol.1700141. [PubMed: 28533444]

Newman R, and Tolar P (2021). Chronic calcium signaling in $IgE^+$ B cells limits plasma cell differentiation and survival. Immunity 54, 2756–2771.e10. 10.1016/j.immuni.2021.11.006. [PubMed: 34879220]

Noble A, and Zhao J (2016). Follicular helper T cells are responsible for IgE responses to Der p 1 following house dust mite sensitization in mice. Clin. Exp. Allergy 46, 1075–1082. 10.1111/cea.12750. [PubMed: 27138589]

Orgel K, and Kulis M (2018). A mouse model of peanut allergy induced by sensitization through the gastrointestinal tract. In Type 2 Immunity, Reinhardt RL, ed. (Springer New York), pp. 39–47.

Ritvo PG, Saadawi A, Barennes P, Quiniou V, Chaara W, El Soufi K, Bonnet B, Six A, Shugay M, Mariotti-Ferrandiz E, and Klatzmann D (2018). High-resolution repertoire analysis reveals a major bystander activation of Tfh and Tfr cells. Proc. Natl. Acad. Sci. USA 115, 9604–9609. 10.1073/pnas.1808594115. [PubMed: 30158170]

Robinson MJ, Prout M, Mearns H, Kyle R, Camberis M, Forbes-Blom EE, Paul WE, Allen CDC, and Le Gros G (2017). IL-4 haploinsufficiency specifically impairs IgE responses against allergens in mice. J. Immunol 198, 1815–1822. 10.4049/jimmunol.1601434. [PubMed: 28115531]

Roco JA, Mesin L, Binder SC, Nefzger C, Gonzalez-Figueroa P, Canete PF, Ellyard J, Shen Q, Robert PA, Cappello J, et al. (2019). Class-switch recombination occurs infrequently in germinal centers. Immunity 51, 337–350.e7. 10.1016/j.immuni.2019.07.001. [PubMed: 31375460]

Satitsuksanoa P, Daanje M, Akdis M, Boyd SD, and van de Veen W (2021). Biology and dynamics of B cells in the context of IgE-mediated food allergy. Allergy 76, 1707–1717. 10.1111/all.14684. [PubMed: 33274454]

Saunders SP, Ma EGM, Aranda CJ, and Curotto de Lafaille MA (2019). Non-classical B cell memory of allergic IgE responses. Front. Immunol 10, 715. 10.3389/fimmu.2019.00715. [PubMed: 31105687]

Shalev I, Liu H, Koscik C, Bartczak A, Javadi M, Wong KM, Maknojia A, He W, Liu MF, Diao J, et al. (2008). Targeted deletion of *fgl2* leads to impaired regulatory T cell activity and development of autoimmune glomerulonephritis. J. Immunol 180, 249–260. 10.4049/jimmunol.180.1.249. [PubMed: 18097026]

Shimoda K, van Deursent J, Sangster MY, Sarawar SR, Carson RT, Tripp RA, Chu C, Quelle FW, Nosaka T, Vignali DAA, et al. (1996). Lack of IL-4-induced Th2 response and IgE class switching in mice with disrupted *Stat6* gene. Nature 380, 630–633. 10.1038/380630a0. [PubMed: 8602264]

Shulman Z, Gitlin AD, Targ S, Jankovic M, Pasqual G, Nussenzweig MC, and Victora GD (2013). T follicular helper cell dynamics in germinal centers. Science 341, 673–677. 10.1126/science.1241680. [PubMed: 23887872]

Sungnak W, Wagner A, Kowalczyk MS, Bod L, Kye YC, Sage PT, Sharpe AH, Sobel RA, Quintana FJ, Rozenblatt-Rosen O, et al. (2020). T follicular regulatory cell-derived Fibrinogen-like protein 2 regulates production of autoantibodies and induction of systemic autoimmunity. J. Immunol 205, 3247–3262. 10.4049/jimmunol.2000748. [PubMed: 33168576]

Talay O, Yan D, Brightbill HD, Straney EEM, Zhou M, Ladi E, Lee WP, Egen JG, Austin CD, Xu M, and Wu LC (2012). IgE+ memory B cells and plasma cells generated through a germinal-center pathway. Nat. Immunol 13, 396–404. 10.1038/ni.2256. [PubMed: 22366892]

Tordesillas L, Berin MC, and Sampson HA (2017). Immunology of food allergy. Immunity 47, 32–50. 10.1016/j.immuni.2017.07.004. [PubMed: 28723552]

Turqueti-Neves A, Otte M, Schwartz C, Schmitt MER, Lindner C, Pabst O, Yu P, and Voehringer D (2015). The extracellular domains of IgG1 and T Cell-derived IL-4/IL-13 are critical for the polyclonal memory IgE response in vivo. PLoS Biol. 13, e1002290. 10.1371/journal.pbio.1002290. [PubMed: 26523376]

Victora GD, and Nussenzweig MC (2012). Germinal centers. Annu. Rev. Immunol 30, 429–457. 10.1146/annurev-immunol-020711-075032. [PubMed: 22224772]

Wade-Vallance AK, and Allen CDC (2021). Intrinsic and extrinsic regulation of IgE B cell responses. Curr. Opin. Immunol 72, 221–229. 10.1016/j.coi.2021.06.005. [PubMed: 34216934]

Wan Z, Lin Y, Zhao Y, and Qi H (2019). $T_{FH}$ cells in bystander and cognate interactions with B cells. Immunol. Rev 288, 28–36. 10.1111/imr.12747. [PubMed: 30874359]

Wang J, Vuitton DA, Müller N, Hemphill A, Spiliotis M, Blagosklonov O, Grandgirard D, Leib SL, Shalev I, Levy G, et al. (2015). Deletion of Fibrinogen-like protein 2 (FGL-2), a novel CD4+ CD25+ Treg effector molecule, leads to improved control of Echinococcus multilocularis Infection in Mice. PLoS Negl. Trop. Dis 9, e0003755. 10.1371/journal.pntd.0003755. [PubMed: 25955764]

Wesemann DR, Magee JM, Boboila C, Calado DP, Gallagher MP, Portuguese AJ, Manis JP, Zhou X, Recher M, Rajewsky K, et al. (2011). Immature B cells preferentially switch to IgE with increased direct Sm to Sμ recombination. J. Exp. Med 208, 2733–2746. 10.1084/jem.20111155. [PubMed: 22143888]

Wu H, Chen Y, Liu H, Xu LL, Teuscher P, Wang S, Lu S, and Dent AL (2016). Follicular regulatory T cells repress cytokine production by follicular helper T cells and optimize IgG responses in mice. Eur. J. Immunol 46, 1152–1161. 10.1002/eji.201546094. [PubMed: 26887860]

Wu YL, Stubbington MJ, Daly M, Teichmann SA, and Rada C (2017). Intrinsic transcriptional heterogeneity in B cells controls early class switching to IgE. J. Exp. Med 214, 183–196. 10.1084/jem.20161056. [PubMed: 27994069]

Xie MM, Chen Q, Liu H, Yang K, Koh B, Wu H, Maleki SJ, Hurlburt BK, Cook-Mills J, Kaplan MH, and Dent AL (2020). T follicular regulatory cells and IL-10 promote food antigen-specific IgE. J. Clin. Invest 130, 3820–3832. 10.1172/JCI132249. [PubMed: 32255767]

Xie MM, Fang S, Chen Q, Liu H, Wan J, and Dent AL (2019). Follicular regulatory T cells inhibit the development of granzyme B-expressing follicular helper T cells. JCI Insight 4, e128076. 10.1172/jci.insight.128076.

Xiong H, Dolpady J, Wabl M, Curotto de Lafaille MA, and Lafaille JJ (2012). Sequential class switching is required for the generation of high affinity IgE antibodies. J. Exp. Med 209, 353–364. 10.1084/jem.20111941. [PubMed: 22249450]

Yang Z, Robinson MJ, and Allen CDC (2014). Regulatory constraints in the generation and differentiation of IgE-expressing B cells. Curr. Opin. Immunol 28, 64–70. 10.1016/j.coi.2014.02.001. [PubMed: 24632082]

Yang Z, Sullivan BM, and Allen CD (2012). Fluorescent in vivo detection reveals that IgE+ B cells are restrained by an intrinsic cell fate predisposition. Immunity 36, 857–872. 10.1016/j.immuni.2012.02.009. [PubMed: 22406270]

Yang Z, Wu CAM, Targ S, and Allen CDC (2020). IL-21 is a broad negative regulator of IgE class switch recombination in mouse and human B cells. J. Exp. Med 217, e20190472. 10.1084/jem.20190472. [PubMed: 32130409]

Yeh C-H, Finney J, Okada T, Kurosaki T, and Kelsoe G (2022). Primary germinal center-resident T follicular helper cells are a physiologically distinct subset of CXCR5$^{hi}$PD-1$^{hi}$ T follicular helper cells. Immunity 55, 272–289.e7. 10.1016/j.immuni.2021.12.015. [PubMed: 35081372]

Yu W, Freeland DMH, and Nadeau KC (2016). Food allergy: immune mechanisms, diagnosis and immunotherapy. Nat. Rev. Immunol 16, 751–765. 10.1038/nri.2016.111. [PubMed: 27795547]

Zhang B, Liu E, Gertie JA, Joseph J, Xu L, Pinker EY, Waizman DA, Catanzaro J, Hamza KH, Lahl K, et al. (2020). Divergent T follicular helper cell requirement for IgA and IgE production to peanut during allergic sensitization. Sci. Immunol 5, eaay2754. 10.1126/sciimmunol.aay2754. [PubMed: 32385053]

## Highlights

- How allergen-specific IgE develops in food allergy is studied using a mouse model
- Production of IgE requires at least two precisely timed allergen exposures
- IgE-expressing B cells in the germinal center require proper timing to proliferate
- Allergen exposure alters the expression of inhibitory factors by helper T cells

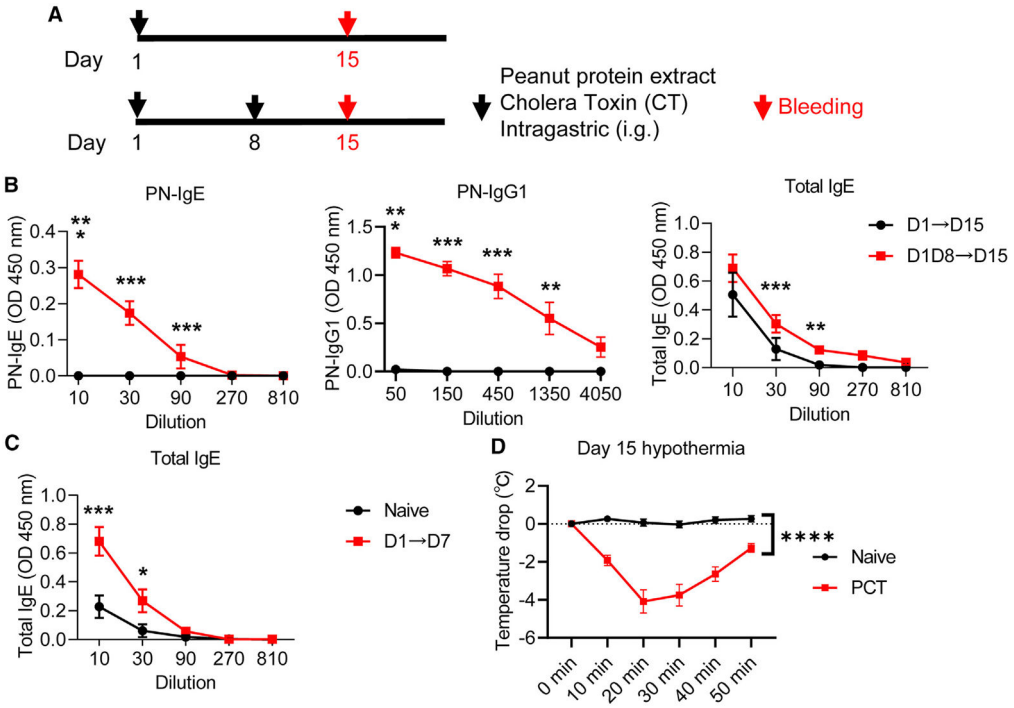


**Figure 1. Development of Ag-specific IgE, but not total IgE, requires a second peanut and cholera toxin (PCT) sensitization**

(A) Schematic figure of the PCT sensitization model.

(B) PN-specific IgE, PN-specific IgG1, and total IgE at the indicated time points after PCT sensitizations. Mice were sensitized with PCT at day 1 or at days 1 and 8, then sera were collected at day 15. n = 4.

(C) Total IgE in naive mice and mice after PCT sensitization. n = 5.

(D) Anaphylaxis reaction after PCT sensitizations. Naive and sensitized mice were injected with 2 mg peanut protein (intraperitoneally [i.p.]) at day 15. n = 7.

*p < 0.05; **p < 0.01; ***p < 0.001; ****p < 0.0001 by two-way ANOVA. Data are representative of two independent experiments. Data are mean ± SEM.

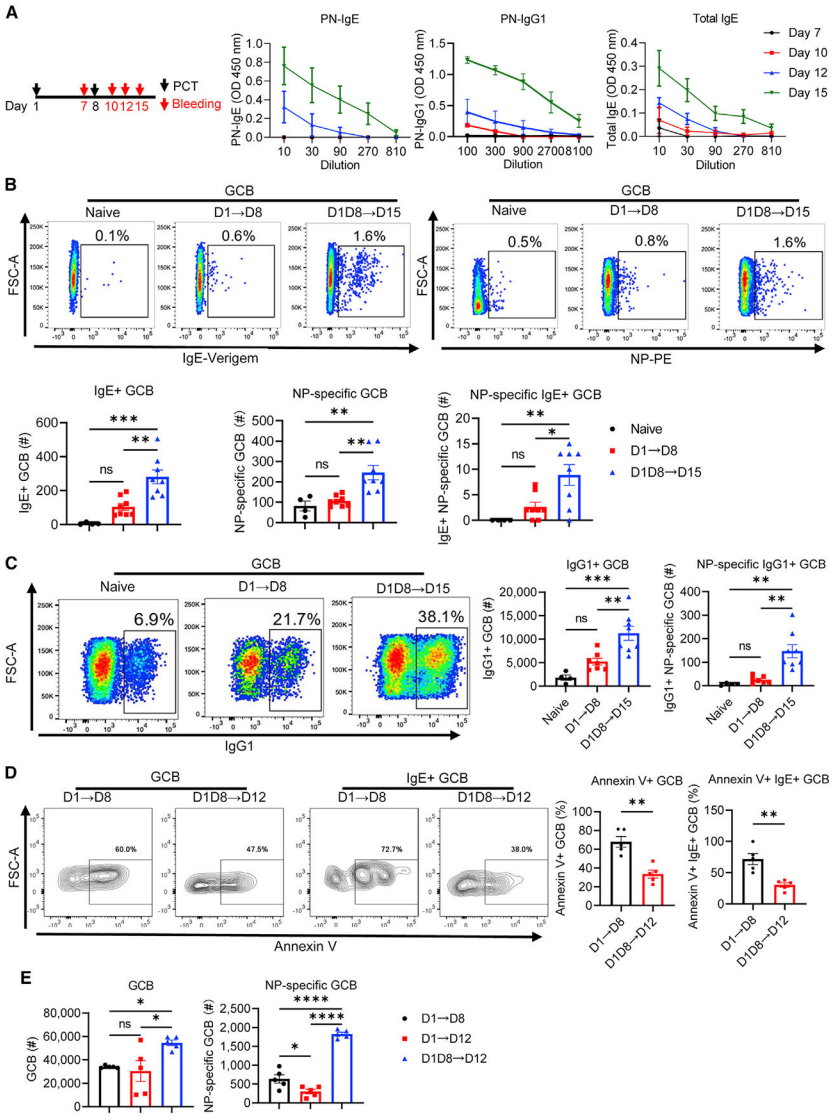


**Figure 2. Second sensitization maintains the expansion of Ag-specific GC B cells and IgE+ GC B cells and inhibits apoptosis**

(A) Development of PN-specific IgE after days 1 and 8 sensitizations. Mice were sensitized with PCT at days 1 and 8. PN-specific IgE, PN-specific IgG1, and total IgE were determined at the indicated time points. n = 4.

(B) NP-specific IgE+ GC B cells before and after second sensitization. Verigem mice were sensitized with NP-OVA + CT at day 1 or days 1 and 8. IgE+ GC B cells and NP-specific GC B cells were analyzed at the indicated time points. Cell number was calculated per mesenteric lymph node (mLN). n = 4 or 8.

(C) NP-specific IgG1+ GC B cells before and after second sensitization. Verigem mice were sensitized with NP-OVA + CT at day 1 or days 1 and 8. IgG1+ GC B cells and NP-specific GC B cells were analyzed at the indicated time points. Cell number was calculated per mLN. n = 4 or 8.

(D) Apoptosis of GC B cells and IgE+ GC B cells. Mice were sensitized with PCT at day 1 or days 1 and 8. Annexin V-positive GC B cells and IgE+ GC B cells were analyzed. n = 5.

(E) GC B cells and NP-specific GC B cells with and without second sensitization. Mice were sensitized with NP-OVA + CT at day 1 or days 1 and 8. GC B cells and NP-specific GC B cells were analyzed at the indicated time points. Cell number was calculated per mLN. n = 5.

*p < 0.05; **p < 0.01; ***p < 0.001; ****p < 0.0001 by one-way ANOVA. ns, not significant. Data are representative of two independent experiments. Data are mean ± SEM.

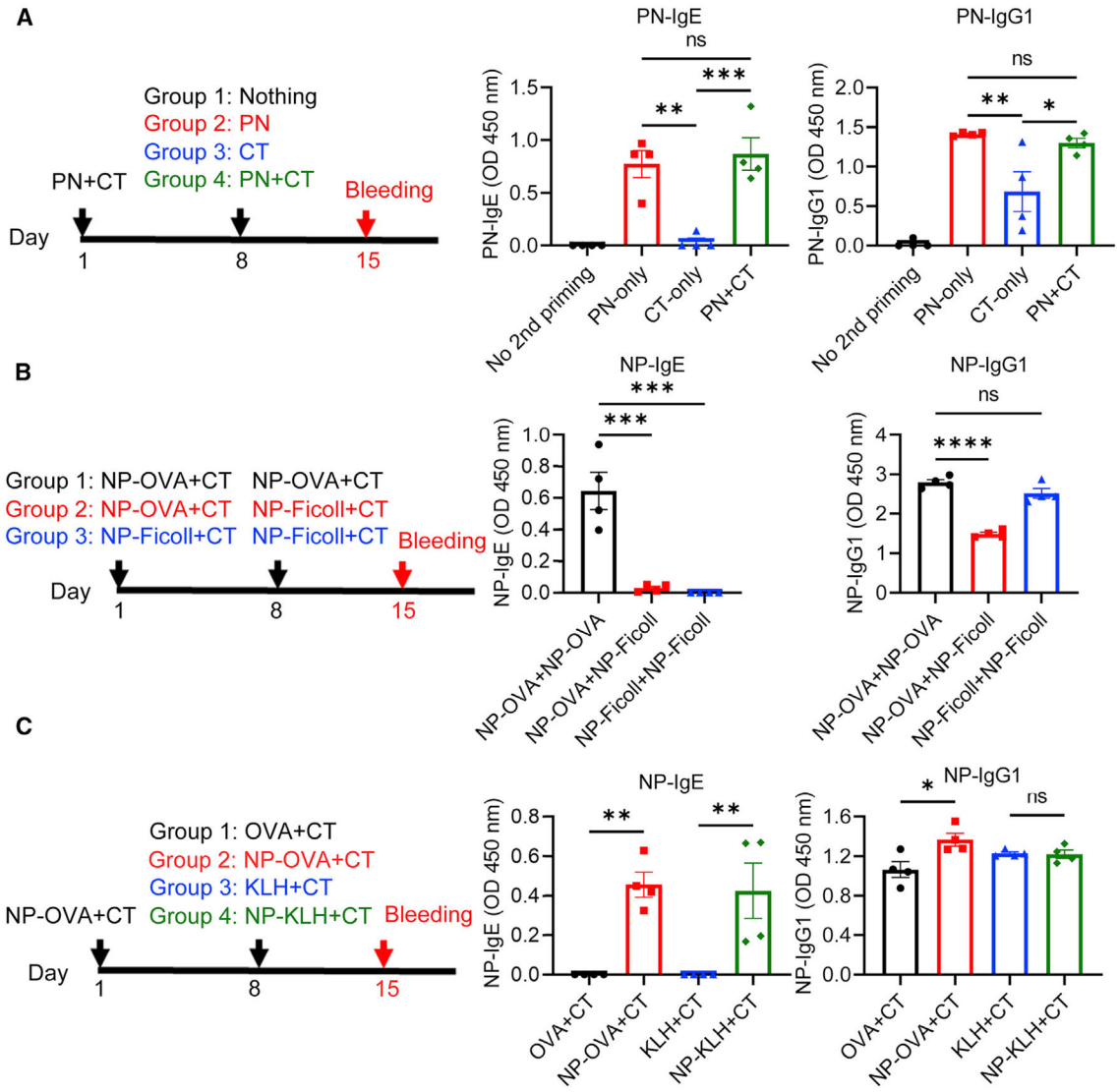


**Figure 3. Development of PN-specific IgE, but not IgG1, is dependent on T cells and stimulation of Ag-specific B cells at second sensitization**

(A) Mice were sensitized with PCT at day 1. These mice were secondarily sensitized with nothing, PN, CT, or PCT at day 8. PN-specific IgE and PN-specific IgG1 were analyzed. n = 4.

(B) Mice were sensitized with different recombination of NP-OVA and NP-Ficoll plus CT at days 1 and 8. NP-specific IgE and NP-specific IgG1 were analyzed. n = 4.

(C) Mice were sensitized with NP-OVA + CT at day 1. These mice were secondarily sensitized with different antigens plus CT as indicated at day 8. NP-specific IgE and NP-specific IgG1 were analyzed by ELISA. Sera dilutions for optical densities (ODs) in graphs: PN-IgE at 1:10; PN-IgG1 at 1:50. n = 4.

*p < 0.05; **p < 0.01; ***p < 0.001; ****p < 0.0001 by one-way ANOVA. ns, not significant. Data are representative of two independent experiments. Data are mean ± SEM.

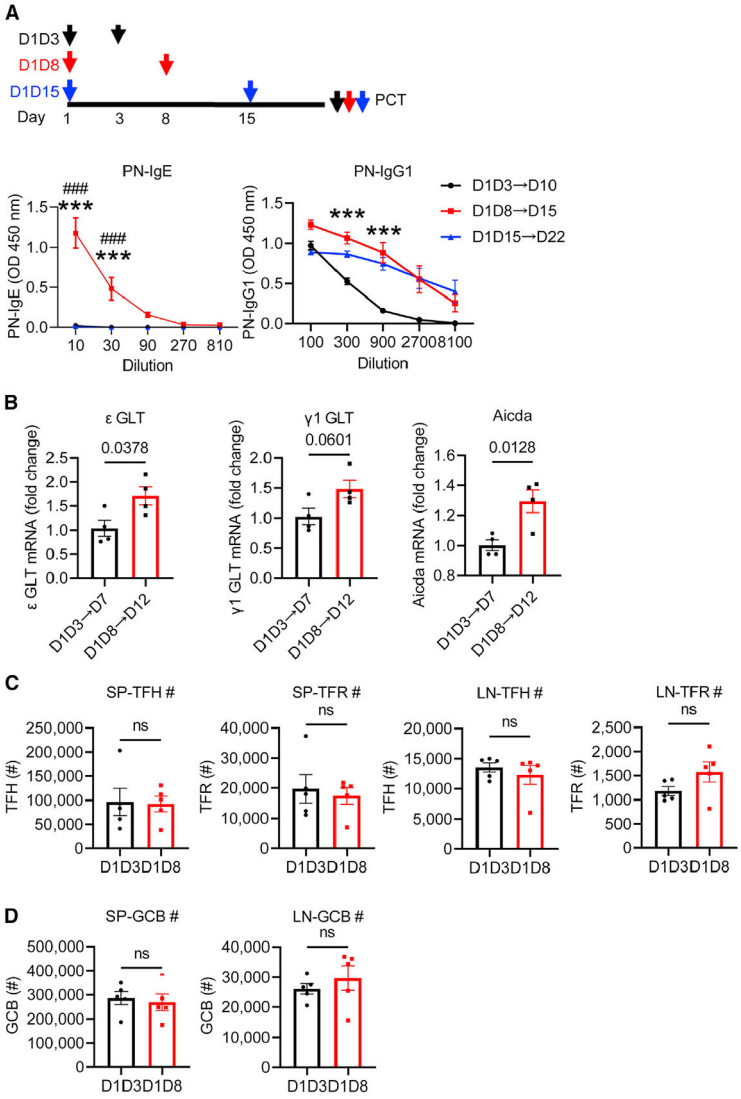


**Figure 4. Development of Ag-specific IgE, but not IgG1, requires proper timing of second sensitization**

(A) Levels of PN-specific IgE, PN-specific IgG1, and total IgE at the indicated time points after different timing of PCT. n = 4. Asterisk (*) represents comparison between days 1 and 8 group and days 1 and 3 group; hash (#) represents comparison between days 1 and 8 group and days 1 and 15 group.

(B) Expression of GLTs and Aicda after PCT sensitizations at days 1 and 3 and days 1 and 8 in total B cells. n = 4.

(C) Numbers of TFH and TFR cells in spleen and mLN after PCT at days 1 and 3 or days 1 and 8. n = 5. Cell number was calculated per spleen or mLN.

(D) GC B cells in spleen and mLN after PCT at days 1 and 3 or days 1 and 8. Cell number was calculated per spleen or mLN. n = 5.

*p < 0.05; **p < 0.01; ***p < 0.001 by two-way ANOVA (A) or t test (B–D). ns, not significant. Data are representative of two independent experiments. Data are mean ± SEM.

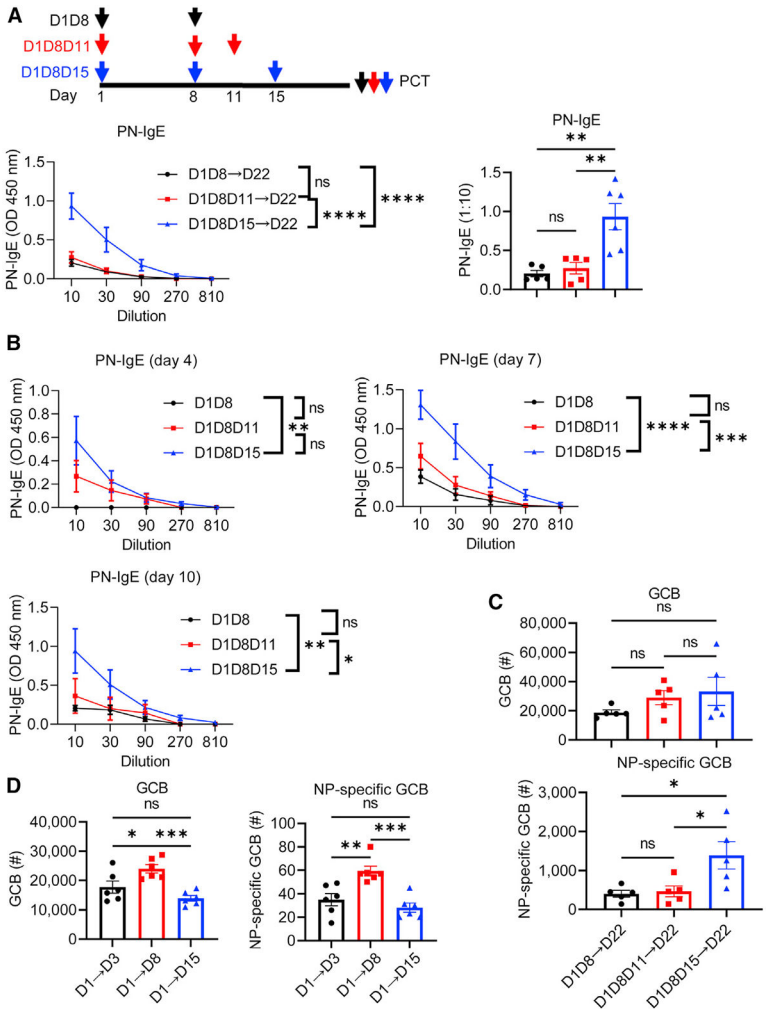


**Figure 5. Properly timed expansion of GC B cells is required for the development of anti-specific IgE**

(A) Levels of PN-specific IgE at day 22 after different timing of PCT. n = 5 or 6.

(B) Levels of PN-specific IgE at 4, 7, and 10 days (separate titration graphs) after different timings of PCT. n = 4 or 5.

(C) GCB and NP-specific GC B cells at day 22 after different timing of PCT. Cell number was calculated per mLN. n = 5.

(D) GC B cells and NP-specific GC B cells at different time points after just one sensitization. Cell number was calculated per mLN. n = 6.

*p < 0.05; **p < 0.01; ***p < 0.001; ****p < 0.0001 by t test (A, C, and D) or two-way ANOVA (A and B). Data are representative of two independent experiments. ns, not significant. Data are mean ± SEM.

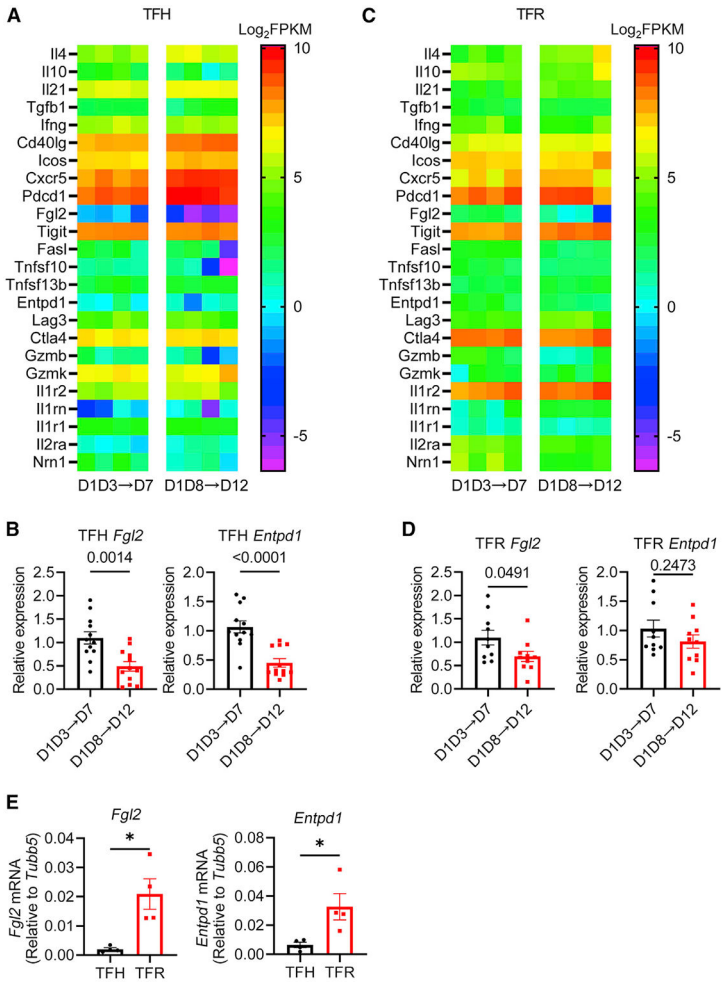


**Figure 6. TFH and TFR gene expression is altered by the timing of antigen sensitization**

(A) Heatmap of selected genes from bulk RNA-seq. TFH cells were sorted 4 days after PCT sensitizations at days 1 and 3 and days 1 and 8. Total RNA was extracted and subjected to bulk RNA-seq and analysis. The heatmap represents the values of $\log_2$FPKM.

(B) mRNA Expression of *Fgl2* and *Entpd1* in TFH cells after PCT at days 1 and 3 and days 1 and 8. Mice were sensitized with PCT at days 1 and 3 and days 1 and 8. TFH cells were sorted at the indicated time points. n = 12.

(C) TFR cells were sorted and used for bulk RNA-seq after PCT sensitizations at days 1 and 3 and days 1 and 8. Total RNA was extracted and subjected to bulk RNA-seq and analysis. The heatmap represents the values of $\log_2$FPKM.

(D) mRNA Expression of *Fgl2* and *Entpd1* in TFR cells after PCT at days 1 and 3 and days 1 and 8. Mice were sensitized with PCT at days 1 and 3 and days 1 and 8. TFR cells were sorted at the indicated time points. n = 10.

(E) Comparison of *Fgl2* and *Entpd1* mRNA expression in TFH and TFR cells. Expression is relative to beta-5 tubulin (*Tubb5*). Mice were sensitized with PCT at days 1 and 3 and days 1 and 8. TFR cells were sorted at the indicated time points. n = 4.

*p < .05 by t test. ns, not significant. Data are combined from three independent experiments (B–D) or representative of two or three independent experiments (E). Data are mean ± SEM.

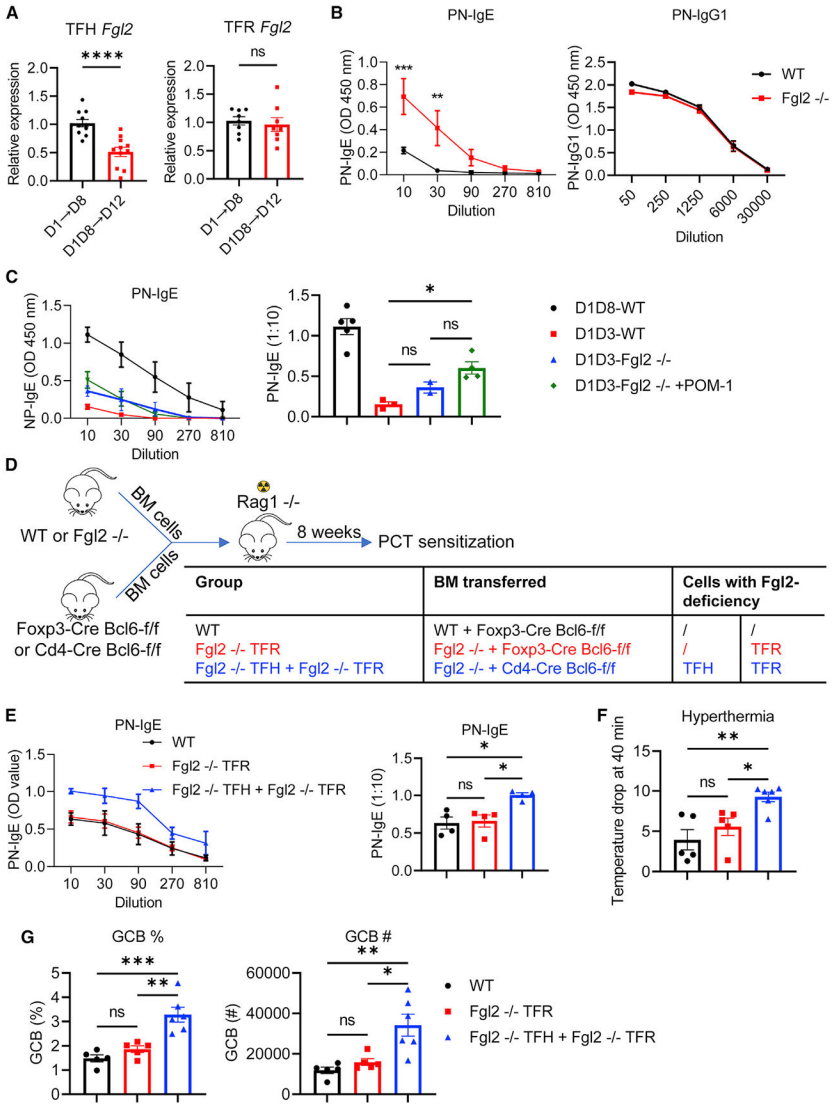


**Figure 7. TFH-cell-derived FGL2 inhibits antigen-specific IgE**

(A) mRNA expression of *Fgl2* in TFH and TFR cells after PCT at the indicated time points. Mice were sensitized with one or two PCT. TFH and TFR cells were sorted at the indicated time points. n = 8 or 11.

(B) Peanut-specific IgE and peanut-specific IgG1 after PCT at days 1 and 8 in WT and *Fgl2*$^{-/-}$ mice. n = 4.

(C) PN-specific IgE in WT mice or *Fgl2*$^{-/-}$ mice with or without POM-1 treatment after PCT at days 1 and 3. n = 2–5.

(D) Scheme of bone marrow chimera mice.

(E) Peanut-specific IgE in bone marrow chimera mice after two PCT sensitizations. *Rag1*$^{-/-}$ recipient mice received bone marrow from WT or *Fgl2*$^{-/-}$ mice in combination with Cd4-Cre Bcl6-fl/fl mice or Foxp3-Cre Bcl6-fl/fl (Bcl6FC) mice. Bone marrow chimera mice were sensitized with PCT at days 1 and 8. PN-specific IgE was determined. n = 5 or 6.

(F) Anaphylaxis reaction in bone marrow chimera mice. Bone marrow chimera mice were injected with 2 mg peanut protein (i.p.) at day 15 after two PCT sensitizations. Body temperature was monitored for 40 min post peanut challenge. n = 5 or 6.
(G) GC B cells in bone marrow chimera mice after two PCT sensitizations. Cell number was calculated per mLN. n = 5 or 6.
*p < 0.05; **p < 0.01; ***p < 0.001; ****p < 0.0001 by t test (A), one-way ANOVA (C and E–G), or two-way ANOVA (B). ns, not significant. Data are combined from two independent experiments (A) or representative of two or three independent experiments. Data are mean ± SEM.

## KEY RESOURCES TABLE

| REAGENT or RESOURCE | SOURCE | IDENTIFIER |
|---|---|---|
| Antibodies | | |
| PE anti-mouse CD185 (CXCR5) Antibody | Biolegend | Cat#145504; RRID: AB_2561968 |
| APC anti-mouse CD279 (PD-1) Antibody | Biolegend | Cat#135210; RRID: AB_2159183 |
| PerCP/Cyanine5.5 anti-mouse CD4 Antibody | Biolegend | Cat#100540; RRID: AB_893326 |
| Pacific Blue™ anti-mouse CD38 Antibody | Biolegend | Cat#102720; RRID: AB_10613468 |
| PerCP/Cyanine5.5 anti-mouse/human CD45R/B220 Antibody | Biolegend | Cat#103236; RRID: AB_893354 |
| APC anti-mouse/human GL7 Antigen (T and B cell Activation Marker) Antibody | Biolegend | Cat#144618; RRID: AB_2800675 |
| FITC anti-mouse IgG1 Antibody | Biolegend | Cat#406606; RRID: AB_493293 |
| Pacific Blue™ anti-mouse FOXP3 Antibody | Biolegend | Cat#126410; RRID: AB_2105047 |
| PE Annexin V | Biolegend | Cat#640908; RRID: AB_2561298 |
| Rat anti Mouse IgE Heavy Chain | BIO-RAD | Cat#MCA419 |
| Biotin Rat Anti-Mouse IgG1 | BD | Cat#553441; RRID: AB_394861 |
| Purified Rat Anti-Mouse IgE | BD | Cat#553413; RRID: AB_394846 |
| Biotin Rat Anti-Mouse IgE | BD | Cat#553419; RRID: AB_394850 |
| Chemicals, peptides, and recombinant proteins | | |
| Peanut protein extract | Greer Laboratories | Patent: XPF171D3A25 |
| OVA | Sigma | Cat#A5503 |
| KLH | Sigma | Cat#H7017-20MG |
| NP-OVA | BIOSEARCH | Cat#N-5051-100 |
| NP-KLH | BIOSEARCH | Cat#N-5060-25 |
| NP-PE | BIOSEARCH | Cat#N-5070-1 |
| Cholera toxin | Sigma | Cat#C8052-2MG |
| Critical commercial assays | | |
| B Cell Isolation Kit, mouse | Miltenyi | Cat#130-090-862 |
| CD4+ T Cell Isolation Kit, mouse | Miltenyi | Cat#130-104-454 |
| Nunc-immuno MicroWell 96 well solid plates | Sigma | Cat#M9410 |
| Pierce Streptavidin Poly-HRP | Thermo Fisher Scientific | Cat#21140 |
| Avidin HRP | Invitrogen | Cat#18-4100-94 |
| TMB Substrate Reagent Set | BD | Cat#555214 |
| Fixation/Permeabilization Solution Kit | BD | Cat#555028 |
| Annexin V Binding Buffer | Biolegend | Cat#422201 |
| TaqMan Fast Advanced Master Mix | Thermo Fisher Scientific | Cat#4444963 |
| Deposited data | | |
| RNA-sequencing | This study | GSE202713 |
| Experimental models: Organisms/strains | | |
| Mouse Foxp3-Cre Bcl6-flox (Bcl6FC) | Alexander Dent | Indiana University School of Medicine |
| Cd4-Cre Bcl6-flox (Bcl6 cKO) | Alexander Dent | Indiana University School of Medicine |
| *Igh*-7$^{tm1.2Cdca}$ (Verigem) | Chris Allen | University of California, San Francisco |
| *Fgl2* knockout (*Fgl2*$^{-/-}$) | Gary A. Levy | University of Toronto |

| REAGENT or RESOURCE | SOURCE | IDENTIFIER |
|---|---|---|
| C.129-*Il4*$^{tm1Lky/J}$(4get) | The Jackson Laboratory | Stock #004190 |
| Oligonucleotides | | |
| *Il4* | Mm00445259 | Thermo Fisher Scientific |
| *Il21* | Mm00517640 | Thermo Fisher Scientific |
| *Il10* | Mm00439614 | Thermo Fisher Scientific |
| *Ifng* | Mm01168134 | Thermo Fisher Scientific |
| *Cd40lg* | Mm00441911 | Thermo Fisher Scientific |
| *Fgl2* | Mm00433327 | Thermo Fisher Scientific |
| *Entpd1* | Mm00515448 | Thermo Fisher Scientific |
| *Aicda* | Mm01184115 | Thermo Fisher Scientific |
| *Tubb5* | Mm00495806 | Thermo Fisher Scientific |
| Software and algorithms | | |
| FlowJo (version 10.6) | TreeStar | https://www.flowjo.com/ |
| Graphpad Prism (version 9) | GraphPad | https://www.graphpad.com/ |